

Mediterranean Marine Science

Vol 23, No 1 (2022)

VOL 23, No 1 (2022)



Patterns of microphytoplankton biomass and diversity in the southern Alboran Sea

HAJAR IDMOUSSI, KARIM HILMI, SAID CHARIB, TARIK BAIBAI, OMAR ETTAHIRI, AHMED MAKAOUI, LAURA ARIN, MARTA ESTRADA, MOHAMED LAABIR, HERVÉ DEMARCQ, FRANCESC PETERS, LAILA SOMOUE, AHMED ERRHIF

doi: [10.12681/mms.27555](https://doi.org/10.12681/mms.27555)

To cite this article:

IDMOUSSI, H., HILMI, K., CHARIB, S., BAIBAI, T., ETTAHIRI, O., MAKAOUI, A., ARIN, L., ESTRADA, M., LAABIR, M., DEMARCQ, H., PETERS, F., SOMOUE, L., & ERRHIF, A. (2022). Patterns of microphytoplankton biomass and diversity in the southern Alboran Sea. *Mediterranean Marine Science*, 23(1), 103–114. <https://doi.org/10.12681/mms.27555> (Original work published December 14, 2021)

Patterns of microphytoplankton biomass and diversity in the southern Alboran Sea

Hajar IDMOUSSI^{1,2}, Laila SOMOUE¹, Francesc PETERS³, Hervé DEMARCO⁴, Mohamed LAABIR⁵, Marta ESTRADA³, Laura ARIN³, Ahmed MAKAOUI¹, Omar ETTAHIRI¹, Tarik BAIBAI¹, Said CHARIB¹, Karim HILMI¹ and Ahmed ERRHIF²

¹ Marine Plankton Ecology Laboratory, National Institute of Fisheries Research, Sidi Abderrahmane Avenue, Ain Diab Casablanca, Morocco

² Health and Environment laboratory, Faculty of Sciences Ain Chock, Hassan II University, Casablanca, Morocco

³ Department of Marine Biology and Oceanography, Institute of Marine Sciences (CSIC), Barcelona, Catalunya, Spain

⁴ MARBEC, Montpellier University, CNRS, Ifremer, IRD, Sète, France

⁵ MARBEC, Montpellier University, CNRS, Ifremer, IRD, Montpellier, France

Corresponding author: Hajar IDMOUSSI; hajar.idmoussi@gmail.com

Contributing Editor: Stelios SOMARAKIS

Received: 19 July 2021; Accepted: 13 December 2021; Published online: 28 February 2022

Abstract

The southern Alboran Sea is a highly dynamic region in the Mediterranean. However, there is few data on microphytoplankton which is, an important component of the marine ecosystem. We therefore collected microphytoplankton samples and related the biomass and diversity patterns to ambient variability, considering cross-shore and longitudinal gradients. There was a general eastward decrease in both species richness and biomass, with Cape Three Forks as a transitional point. Diversity increased in coastal areas and decreased with depth. High chlorophyll-a concentrations corresponded to low temperature and low salinity waters, indicating the Atlantic origin. Microphytoplankton biomass was low in comparison with total chlorophyll, suggesting a dominance of nano- and picophytoplankton. Biomass values increased in the stretch between Cape Three Forks and Al Hoceima Bay, an area highly influenced by upwelled water originating from the northern Alboran Sea. We suggest that the Western Alboran Gyre enhances the development of dinoflagellates while local upwelling enhances the development of diatoms. A statistical relationship was found between microphytoplankton biomass and diversity, especially when diversity was estimated as species richness. These results are crucial for understanding microphytoplankton dynamics and trends in an area that is undergoing climate-derived changes and biodiversity losses.

Keywords: Microphytoplankton; Southern Alboran Sea; Diversity; Biomass; Coastal and offshore waters.

Introduction

The Mediterranean Sea is a hotspot of biodiversity (Coll *et al.*, 2010) and a frontier region between subtropical and temperate regimes. However, biodiversity is decreasing globally at rates that are tens to hundreds of times greater than those of palaeontological extinction (Duarte *et al.*, 2006; IPBES, 2019). In the marine environment, large changes in phytoplankton groups have been related to past climate fluctuations (Falkowski & Oliver, 2007), and marine organisms in the Mediterranean Sea are presumably undergoing similar trends in response to climate change. On the other hand, there is a clear expansion of Lessepsian fish species (Arndt & Schemberi, 2015). Also, thermophilic toxic microalgae such as *Gambierdiscus* and *Ostreopsis* seem to be expanding from tropical seas into the Mediterranean (Pavaux *et al.*, 2020; Tester *et*

al., 2020), threatening ecosystem functioning and human health.

Microphytoplankton is one of the major components of the food web in various ecosystems and is often relatively more abundant in high fish production areas. This was made explicitly evident after the construction of the Assuan high dam, when the coastal phytoplankton community off Egypt changed dramatically and diatom blooms decreased, leading to consequent changes in the associated fisheries (Aleem, 1972). Thus, not only total phytoplankton biomass but also the involved microphytoplankton taxa and their relative contributions are of importance. In this context, the concept of diversity may provide an interesting indicator of phytoplankton community properties. According to Margalef (1999), biodiversity comprises all the available taxonomic or genetic units in a given environment, while ecological diversity

(or simply, diversity) expresses the richness of existing species and the relationships of abundance between them and is based on a census of the species or components of a particular community at a given time; it can be estimated using various diversity indices. Margalef (1958) showed a pattern of changing diversity following upwelling events in the Galician rías (NW Spain), where diversity was first lowered during the initial rapid growth response and later increased as the available nutrients diminished. Irigoien *et al.*, 2004 using a marine phytoplankton global dataset, found a diversity peak at intermediate levels of phytoplankton biomass. Furthermore, conditions leading to a larger biomass tend to be associated with a certain environmental variability that favours nutrient availability and system production (Estrada, 1996; Iversen *et al.*, 2010; Scales *et al.*, 2014; Alcaraz *et al.*, 2016). All these aspects require a census of phytoplankton taxa.

To date, little is known about biodiversity or biomass and diversity patterns regarding microphytoplankton in the southern Mediterranean (Mercado *et al.*, 2005; Daoudi *et al.*, 2012; Rijal Leblad *et al.*, 2013, 2020; Salhi *et al.*, 2018).

In the present study, we aim to show the patterns of microphytoplankton biomass and diversity along the southern part of the Alboran Sea. This objective is motivated by the particular hydrological status of this Mediterranean region as a dynamic transition area of Atlantic waters entering the Gibraltar strait and mixing with Mediterranean waters. A couple of anticyclonic gyres add to the spatial variability in the area (Vargas-Yáñez *et al.*, 2002), moving upwelled waters from the northern Alboran Sea southward (Gómez-Jakobsen *et al.*, 2019) and generating local upwelling spots along the African coast. This environmental variability makes this region an excellent testing area to highlight functional links between microphytoplankton diversity and biomass. In agreement with Irigoien *et al.*, 2004, we hypothesize that areas with higher hydrodynamic variability accompanied by nutrient input will show a larger biomass and, up to a certain level of biomass, also greater diversity. We also hypothe-

size that littoral areas with a large terrestrial nutrient load favour biomass rather than diversity.

Materials and Methods

Field sampling

A cruise was carried out in April 2018 with the Moroccan oceanographic vessel *Al Amir Moulay Abdallah* in the southern Alboran Sea following the Moroccan coastline from Saïdia (35.17833° N, 2.26333° W) to the Gibraltar Strait at M'diq (35.88333° N, 5.23111° W) for ca. 540 km. Seawater samples were collected with 1.7-L Niskin bottles from two layers: surface (2-5 m) and bottom depending on the maximum depth of the station, which ranged from 20 to 400 m (Fig. 1; Supplementary Table S1). Temperature and salinity were measured with a SB-E911PLUS Sea-Bird CTD. CTD profiles were not taken in all stations (Supplementary Table S1). Moreover, the cruise did not cover the offshore section between Cape Three Forks and Al Hoceïma Bay. To fill these gaps, we used daily data from the Med MFC physical reanalysis product MEDSEA_MULTIYEAR_PHY_006_004, available from Marine Copernicus at <https://resources.marine.copernicus.eu>. This product is based on the Nucleus for European Modelling of the Ocean (NEMO) hydrodynamic model (Escudier *et al.*, 2020).

Chlorophyll *a*

Seawater (500 mL) was filtered through 47 µm Whatman GF/F filters for the analysis of chlorophyll *a* (chl *a*) (Linder, 1974). Chl *a* fluorescence was measured with a calibrated Turner 10-AU fluorometer after pigment extraction with acetone 90%. In addition, remote sensing of chl *a* data were provided from the MODIS sensor at <https://oceancolor.gsfc.nasa.gov> during the same sampling period.

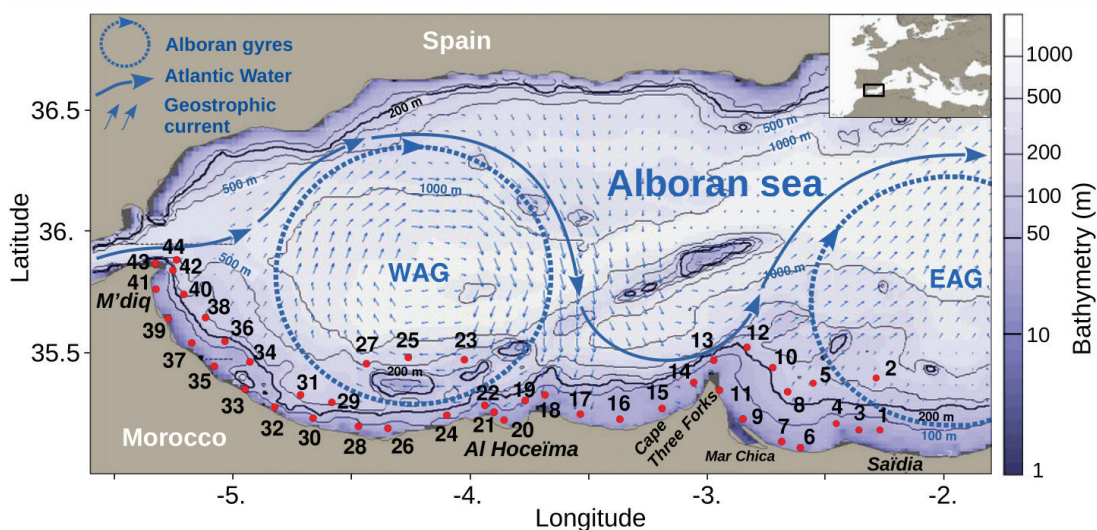


Fig. 1: Bathymetry of the Alboran Sea with the main oceanographic features. WAG and EAG are western and eastern Alboran gyre, respectively. The dots are the stations sampled during the cruise (14 to 26 April 2018). The average geostrophic currents for 17 April 2018 are overlaid.

Phytoplankton Community analysis

Seawater samples for phytoplankton analysis (100 ml) were taken from Niskin bottles and fixed using Lugol's solution. Phytoplankton identification and counts were carried out according to the Utermöhl (1958) method using a Nikon Eclipse Ti inverted microscope at x200. Phytoplankton was determined to the lowest taxonomic level possible. Pictures were taken with a Nikon digital camera. In order to estimate biomass, cell volume (CV, $\mu\text{m}^3 \text{ cell}^{-1}$) was calculated using geometric approximations of shapes (Menden-Deuer & Lessard, 2000; Arin *et al.*, 2002; Vadrucci *et al.*, 2007). Dimensions were measured from pictures using ImageJ (Schneider *et al.*, 2012) and a slide micrometer scaling or were obtained from the literature. Then, biomass as carbon content (CC, pg cell^{-1}) was estimated from allometric equations. For diatoms, we used $\text{CC} = 0.288 \cdot \text{CV}^{0.811}$ (Menden-Deuer & Lessard, 2000). Dinoflagellate carbon was estimated using Pavlovskaya & Kondratyeva (1981) as $\text{CC} = 0.387 \cdot \text{CV}^{0.900}$. Finally, for other phytoplankton groups we used $\text{CC} = 0.216 \cdot \text{CV}^{0.939}$ following Menden-Deuer & Lessard (2000).

Total phytoplankton biomass ($\mu\text{g C L}^{-1}$) was calculated from chlorophyll *a* values using eq. 8 in Sathyendranath *et al.* (2009).

Species richness and Ecological diversity indices for phytoplankton

We calculated the frequency of a species (F_i) as $F_i = n_{si}/N_s \cdot 100$, where n_{si} is the number of samples in which species *i* is present and N_s is the total number of samples (Dajoz, 2000). Several ecological indices related to species diversity were also calculated. Species richness (*S*) is the number of taxa present in each sample. The ecological diversity as expressed by the Shannon index (H') (Shannon & Wiener, 1949) was calculated as

$$H' = \sum_{i=1}^s \frac{n_i}{N} \log_2 \frac{n_i}{N}, \text{ where } s \text{ is the species richness for a}$$

specific sample, n_i is the abundance of taxon *i* and *N* is the total abundance of all taxa in the sample. The Hulbert index for dominance (δ) (Hulbert, 1963) was calculated as $\delta = 100 \left(\frac{n_1 + n_2}{N} \right)$, where n_1 is the abundance of the dominant taxon and n_2 is the abundance of the second most abundant taxon.

The distribution patterns of phytoplankton composition were summarized using principal component analysis (PCA) (Estrada & Blasco, 1979; Estrada, 1982) based on the correlation matrix among selected taxa. The analyses were done with a total of 35 species that fulfilled $F_i > 10\%$. Before computation, data were logarithmically transformed to normalize variance and to reduce the influence of dominant taxa on the ordination. Using Cape Three Forks as a turning point, we further assessed differences between the eastern and western areas. Statistical east-west differences were analysed using the Welch t-test, which accounts for unequal sampling size and variance. The variability between surface and deep

samples was tested using a pairwise comparison. In order to analyse the relationships of diversity (Species richness, Shannon index) with other variables, we used stepwise multiple regression analysis. In this case, we discarded samples below 100 m depth because photosynthetic organisms may be strongly compromised. Variables were log10-transformed when necessary to approximate normal distributions.

Results

The physical environment

The lowest surface temperatures (ca. 15.46°C) were observed between Cape Three Forks and Al Hoceima Bay under the direct influence of the Atlantic jet and the Western Alboran Gyre (Fig. 2A). The highest temperatures (ca. 16.83°C) were observed in the eastern area, with maxima found in front of the Mar Chica Lagoon and between M'diq and Al Hoceima Bay. The surface salinity showed a positive eastward gradient but never exceeded 36.6 (Fig. 2B). The lowest salinity values (ca. 35.9) were characteristic of Atlantic waters.

At coastal stations, the mixed-layer depth reached 80 m between M'diq and Al Hoceima Bay and especially in the east. In the coastal area east of Cape Three Forks, the surface mixed layer depth ranged between 13.2 to 22.3 m (Fig. 2C). The coastal area between Al Hoceima Bay and Cape Three Forks was characterized by cold waters with quickly decreasing vertical temperatures, and salinity increased eastward (Fig. 3). At the offshore stations, temperature decreased with depth in the whole area. In contrast, salinities increased with depth corresponding to salinities characteristic of the Mediterranean Sea (up to 38.5) being observed in deep layers (150-600 m) (Fig. 3).

Chlorophyll *a*

Low concentrations ($<0.2 \mu\text{g L}^{-1}$) of chl *a* (Fig. 4A) were consistently found to the east of Cape Three Forks, while the highest values were recorded between M'diq and the River Oued Laou (35.74083°N , 5.13972°W) and between Cape Three Forks and Al Hoceima Bay, with a maximum of $0.69 \mu\text{g L}^{-1}$.

Furthermore, satellite remote-sensed surface chlorophyll (Suppl. Material Fig. S1) showed the highest concentrations ($>10 \mu\text{g L}^{-1}$) along the Spanish coast in the northern Alboran Sea, while concentrations ranged between 2 and $4 \mu\text{g L}^{-1}$ at coastal stations of the southwestern Alboran Sea, as well as between 3.74444°W and Cape Three Forks. The lowest concentrations characterized the southeastern region east of Cape Three Forks, as confirmed by the *in situ* data. At coastal stations, surface and deep samples had almost the same mean chl *a* concentrations, while at the open sea stations the concentrations were higher at the surface than at depth. Chlorophyll variability was high in the open sea (Table 1).

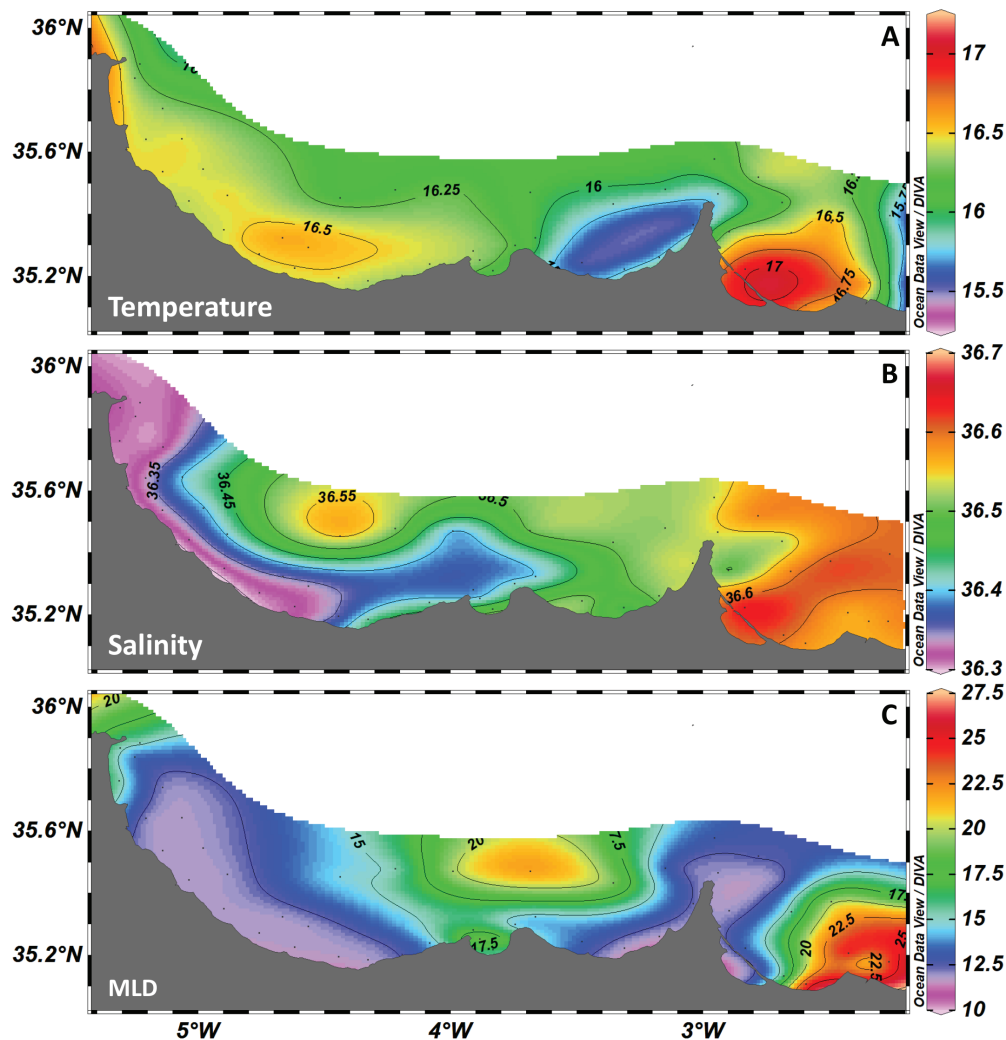


Fig. 2: Spatial distribution of physical parameters. MLD is the ocean mixed-layer thickness calculated as the depth at which the density increases by 0.01 kg m^{-3} compared with the density at 10 m depth. Temperature (A), salinity (B), MLD (C).

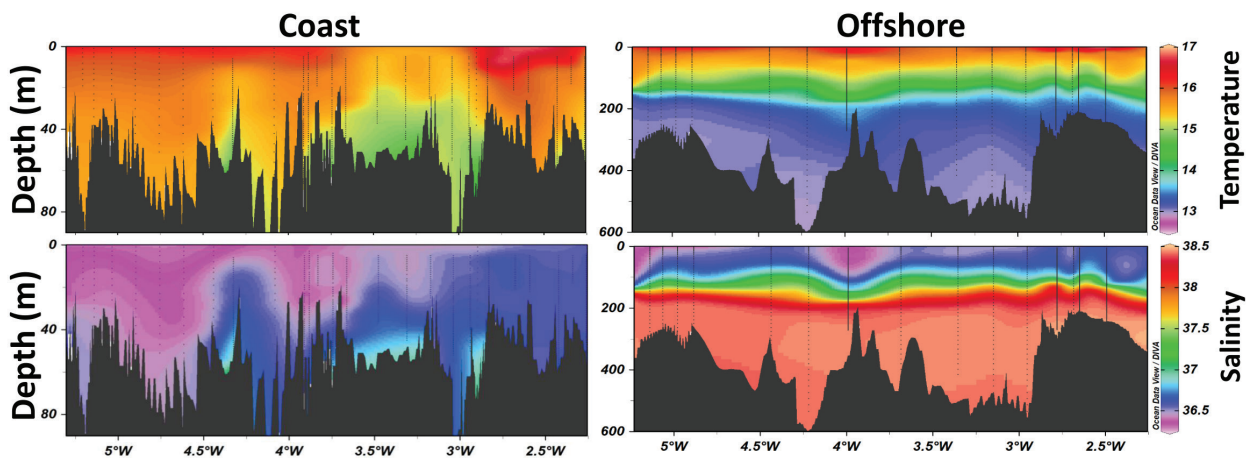


Fig. 3: Longitudinal sections of temperature (upper panels) and salinity (lower panels) along the coast (left panels) and offshore (right panels).

Microphytoplankton composition and biomass

We identified 106 phytoplankton taxa (Supplementary Table S2), mostly belonging to Bacillariophyceae (54 species) and Dinophyceae (48 species). We also identified *Euglena* spp., *Chattonella* spp., *Otonaria* spp. and *Coc-*

colithus spp. which belong to Euglenophyceae, Raphidophyceae, Silicoflagellates and Coccolithophoridae, respectively. The taxa with the highest relative abundances are shown aggregated in Figure 5 and disaggregated for each group (Supplementary Table S3).

Most taxa identified during this oceanographic cruise

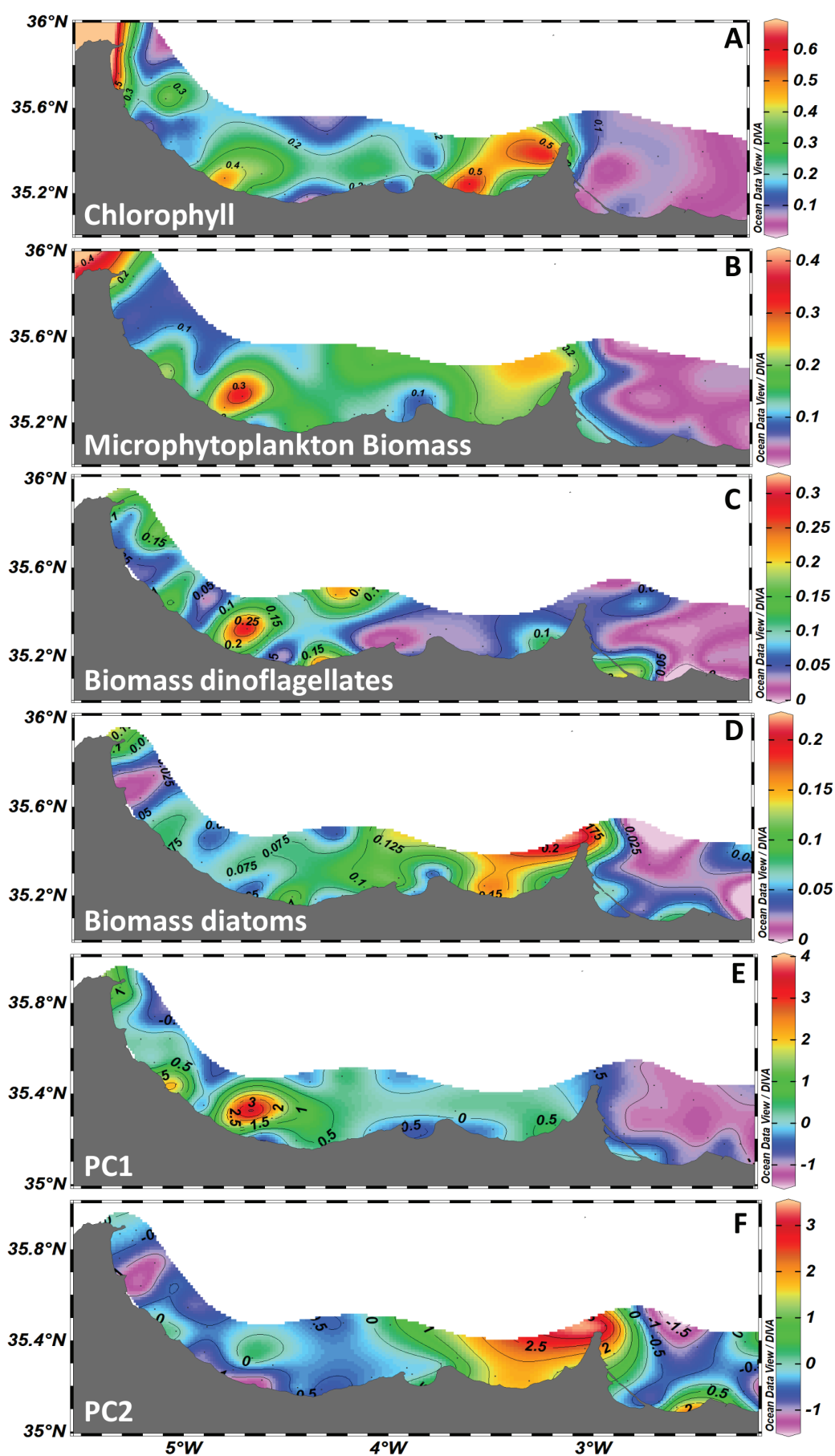


Fig. 4: Surface distribution of variables and properties: A) *in situ* total chlorophyll *a* ($\mu\text{g L}^{-1}$), B) total microphytoplankton biomass ($\mu\text{g C L}^{-1}$), C) dinoflagellate biomass ($\mu\text{g C L}^{-1}$), D) diatom biomass ($\mu\text{g C L}^{-1}$), E) scores from the first component of PCA and F) scores from the second component of PCA.

Table 1. Pairwise comparison between surface and deep samples regarding different variables. There were 28 coastal stations and 16 open-sea stations. Values for surface and deep are means.

Variable	Coastal stations			Open sea stations		
	surface	deep	p-value	surface	deep	p-value
Chl-a	0.226	0.224	0.4800	0.184	0.048	0.0002
Microphytoplankton†	0.146	0.094	0.0008	0.147	0.113	0.3176
Shannon Diversity	2.89	2.56	0.0006	2.90	2.52	0.0142
Richness	18.25	11.86	<.0001	16.56	8.75	0.0008

† Microphytoplankton biomass

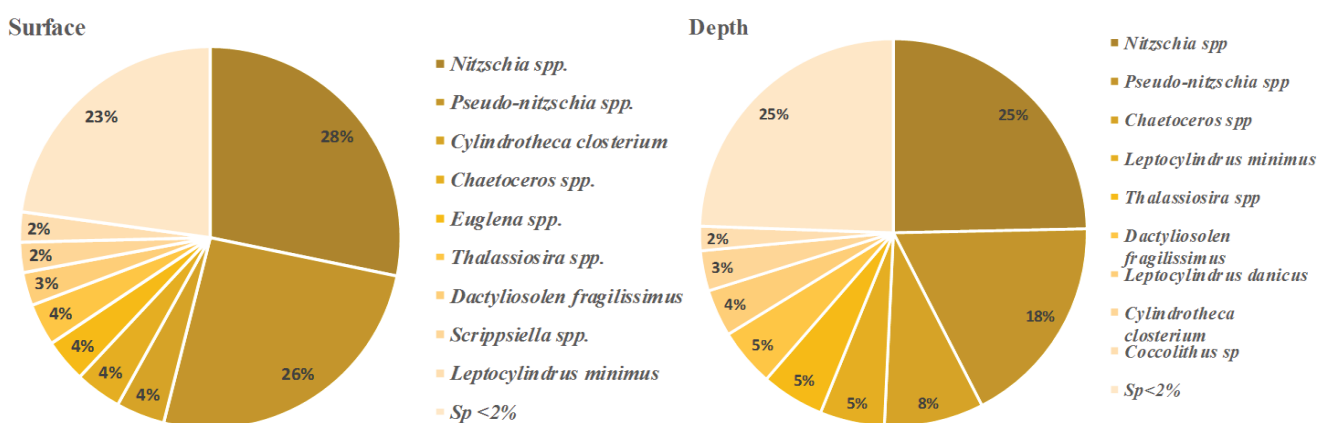


Fig. 5: Relative abundances of the most abundant taxa of all groups of phytoplankton along the southern Alboran sea in April 2018, in surface and deep layers.

are usually found in nearby Atlantic waters (Elghrib *et al.*, 2012; Demarcq & Somoue, 2015), suggesting that the western Mediterranean coast is strongly influenced by Atlantic waters. An exception is *Actiniscus pentasterias*, found in very low abundance during this cruise. *Leptocylindrus mediterraneus* is rarely found in adjacent Atlantic waters, and when it occasionally occurs, its abundance is very low (Somoue *et al.*, unpublished data). The similarity in taxa between the western and the eastern part is 97%. However, the abundance of some taxa, such as *L. mediterraneus*, is very different in these two areas (Supplementary Table S4). Surface waters showed 4.3 % of *L. mediterraneus* east of Cape Three Forks and 0.2 % west of it, while bottom waters showed a 2 % abundance across both areas. These results show that Mediterranean waters characterize deep layers while Atlantic waters, particularly in the west, characterize the surface layer of the southern Alboran Sea, in accordance with the main circulation patterns in the basin. Similarly, *Chaetoceros* spp., *Cylindrotheca closterium* and *Dactyliosolen fragilissimus* show higher abundances to the east of Cape Three Forks and *Nitzschia* spp. and *Pseudo-nitzschia* spp. to the west of it (Supplementary Table S4).

According to the Principal Component Analysis, microphytoplankton taxa showed a longitudinal variability pattern and a low variability between surface and bottom waters. The first three components accounted for 14.9%, 11.2% and 8.4% of the total variance. These proportions are relatively low, reflecting the existence of multiple factors influencing the phytoplankton community in this

particular area. The surface distribution of the scores of the first and second components is shown in Figures 4E and 4F. The highest positive values of the first principal component (PC1) occur in the western area and its spatial pattern is closely related to the dinoflagellates abundances. The species having the highest positive correlations with the first component (in blue in Fig. 6) were *Triplos furca*, *Prorocentrum micans*, *Triplos lineatus*, *Diplopsalis* spp., *Scrippsiella* spp., *Lingulodinium* spp., *Dinophysis acuminata*, *Gymnodinium* spp., *Chattonella* spp., *Euglena* spp. and *Coccolithus* spp. The component (PC2) presents the highest values in the area between Cape Three Forks and Al Hoceima Bay, as influenced by the Western Alboran Gyre and the waters from the northern Alboran Sea, with a spatial pattern similar to that of diatoms. The species having the highest correlations with the second component (in red in Fig. 6) were *Nitzschia longissima*, *Dactyliosolen fragilissimus*, *Chaetoceros* spp., *Helicotheca tamesis*, *Cylindrotheca closterium*, *Leptocylindrus mediterraneus* and *Leptocylindrus minimus*.

Microphytoplankton abundance was important near the surface than in deep layers, especially in the western part from M'diq to Cape Three Forks where densities were higher than 2×10^4 cells L^{-1} and reached a maximum of 2.73×10^4 cells L^{-1} (Fig. 7). At depth, the densities did not exceed 1.5×10^4 cells L^{-1} , except for station 7, with a maximum of 2.02×10^4 cells L^{-1} .

Phytoplankton biomass ranged between 0.10 and 0.42 $\mu g C L^{-1}$, with the highest values being mainly found in the western part of the southern Alboran Sea, from Cape

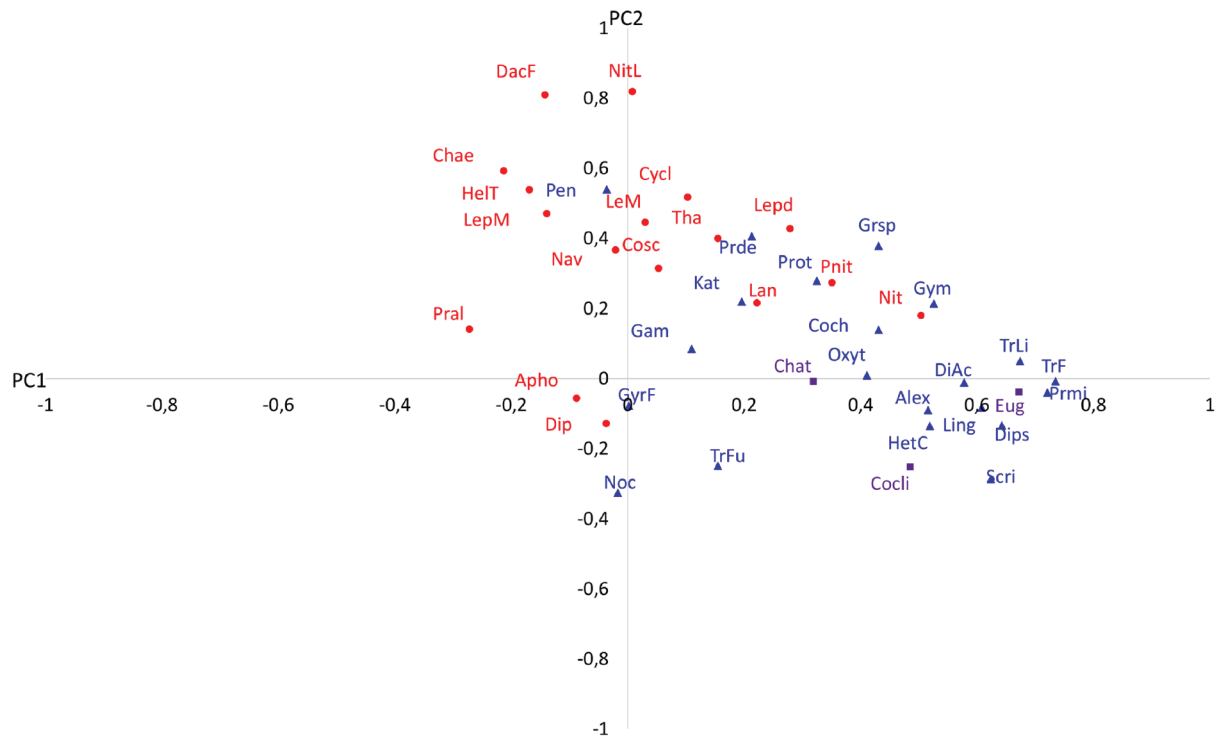


Fig. 6: Position of the 35 species in the space dimensioned by the first and the second principal components of the PCA analysis. Abbreviations: Alex: *Alexandrium* spp.; Apho: *Amphora* spp.; Chae: *Chaetoceros* spp.; Chat: *Chatonella* spp.; Coch: *Cochlodinium* spp.; Cocli: *Coccolithus* spp.; Cosc: *Coscinodiscus* spp.; Cycl: *Cylindrotheca closterium*; DacF: *Dactyliosolen fragilissimus*; DiAc: *Dinophysis acuminata*; Dip: *Diploneis* spp.; Dips: *Diplopsalis* spp.; Eug: *Euglena* spp.; Gam: *Gambierdiscus* spp.; Grsp: *Gyrodinium spirale*; Gym: *Gymnodinium* spp.; GyrF: *Gyrodinium fusus*; HelT: *Helicotheca tamesis*; HetC: *Heterocapsa* spp.; Kat: *Katodinium* spp.; Lan: *Lauderia annulata*; LeM: *Leptocylindrus minimus*; Lepd: *Leptocylindrus danicus*; LepM: *Leptocylindrus mediterraneus*; Ling: *Lingulodinium* spp.; Nav: *Navicula* spp.; Nit: *Nitzschia* spp.; NitL: *Nitzschia longissima*; Noc: *Noctiluca scintillans*; Oxyt: *Oxytoxum* spp.; Pen: *Pentapharsodinium* spp.; Pnit: *Pseudo-nitzschia* spp.; Pral: *Proboscia alata*; Prde: *Proto-peridinium depressum*; Prmi: *Prorocentrum micans*; Prot: *Proto-peridinium* spp.; Scri: *Scrippsiella* spp.; TrLi: *Tripos lineatus*; TrF: *Tripos furca*; TrFu: *Tripos fusus*.

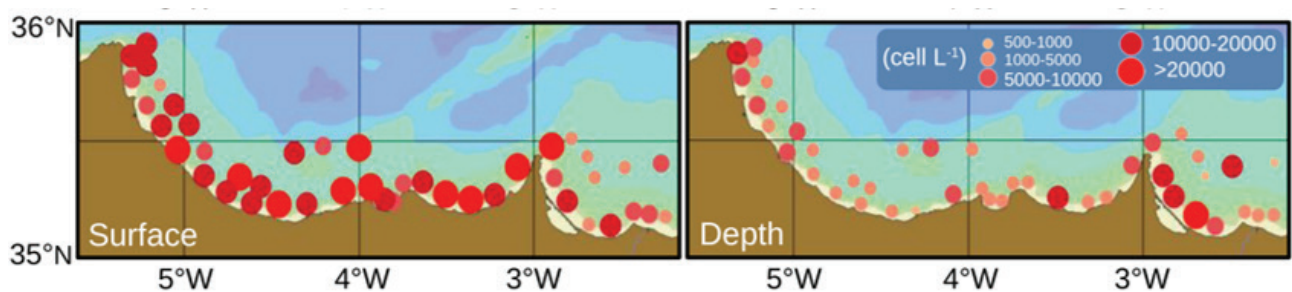


Fig. 7: Spatial distribution of the microphytoplankton abundance (cell L⁻¹) both in the surface and the deep layer.

Three Forks to M'diq (Fig. 4B). As happened with abundance, at most coastal stations, microphytoplankton biomass was higher at surface than at depth. There was a notable exception at station 5 where the biomass in depth was higher 0.42 $\mu\text{g C L}^{-1}$ than the surface 0.028 $\mu\text{g C L}^{-1}$ because of the presence of high number of large cells of the dinoflagellate *Noctiluca scintillans*. In open waters, no statistically significant differences occurred between surface and deep waters (Table 1).

Taxonomical diversity and phytoplankton distribution

Three components of phytoplankton taxonomical diversity were evaluated for the surface distribution: species richness (S), Shannon diversity (H') and dominance. Two regions can be distinguished: an eastern region from

Saïdia to Cape Three Forks with $S < 24$ and a western region from Cape Three Forks to M'diq with $S > 24$ (Fig. 8A). The lowest H' diversity was observed in the western area, where simultaneous blooms of *Nitzschia* spp. and *Pseudo-nitzschia* spp. occurred (Fig. 8B). At the coastal stations, species richness and H' diversity were higher in surface than in deep layers, while in the open sea H' diversity showed no statistical depth differences (Table 1). The areas with high dominance (Fig. 8C) were characterized by low diversity. Furthermore, all indices (except H' diversity) showed significant differences between east and west at the surface, whereas no such difference was found at depth (Table 2).

Species richness was related directly to total micro-

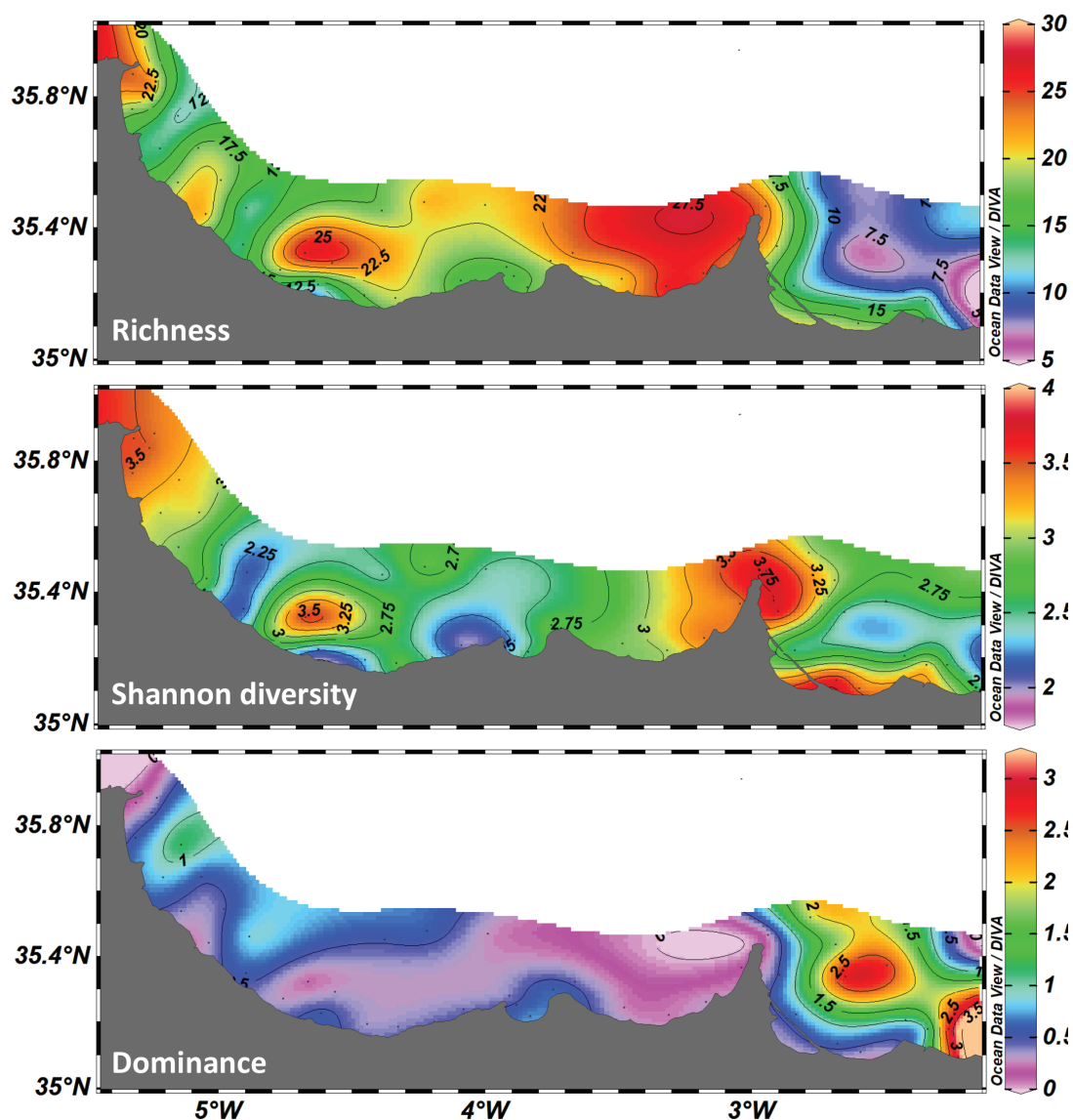


Fig. 8: Surface distribution of diversity indices. Species richness or biodiversity (A), Shannon diversity (B) and Hulbert dominance (C).

Table 2. Summary statistics for east-west comparisons of diversity indices.

		Richness		Shannon		Hulbert	
		West	East	West	East	West	East
Surface	average	19.6	12.3	2.9	3	0.46	1.41
	p-value	<0.001		0.61		0.011	
Depth	average	10.4	11.5	2.5	2.6	1.9	2.48
	p-value	0.61		0.6809		0.3945	

phytoplankton biomass and inversely to sample depth to explain 69 % of total variance in richness data (Fig. 9). The best model for Shannon diversity also included the same variables, as well as a direct relationship with longitude and an inverse relationship with mixed-layer depth.

However, this model only explains a total of 29% of the variability in Shannon diversity, so that a large amount of variability is left unexplained. All in all, the first two variables indicate a direct relationship of diversity to biomass.

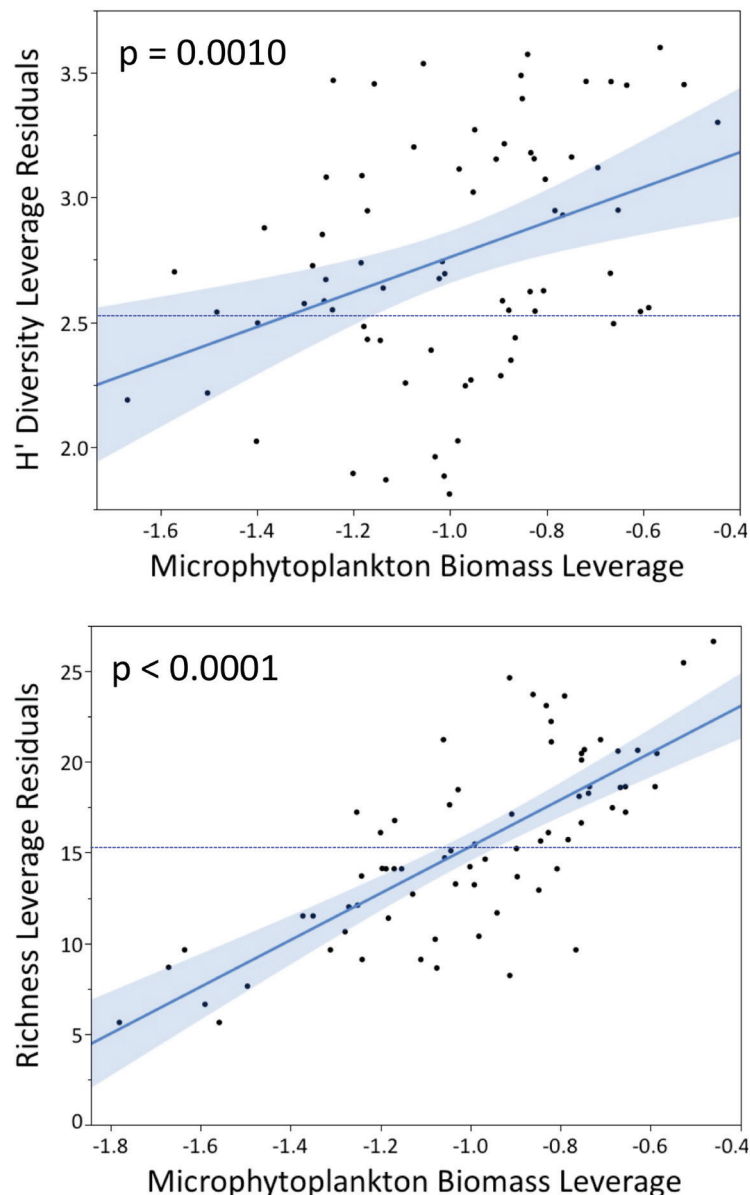


Fig. 9: Leverage plots of the main variable (microphytoplankton biomass) selected into the multiple regression models to explain Shannon diversity and species richness. The shaded area is the confidence interval and the horizontal line is the mean.

Discussion

Microphytoplankton biomass has been considered as a predictor of species richness and Shannon diversity, albeit without the dome-shaped relationship found in Irigoien *et al.*, 2004. In our study, total phytoplankton biomass including pico, nano and microphytoplankton ranged from 2.6 to 51.5 $\mu\text{g C L}^{-1}$, which would correspond to the lower half of the biomass of the unimodal relationship in Irigoien *et al.*, 2004, where the relationship approximates a linear trend.

During our sampling cruise, the biomass of microphytoplankton was low in relation to total chlorophyll, indicating a dominance of smaller organisms, namely nano- and picophytoplankton. This finding corroborates the previous work of Salhi *et al.*, 2018 and stresses the need to investigate these communities in the southern Alboran Sea. The small size fractions of phytoplankton dominate when total phytoplankton biomass is low, whereas large

phytoplanktonic species may dominate when biomass is high in productive waters (Agawin *et al.*, 2000; Irigoien *et al.*, 2004).

The biomass of diatoms increased in the area between Cape Three Forks and Al Hoceima Bay (Fig. 4D), because of the influence of waters from the northern Alboran Sea upwelling. The biomass of dinoflagellates was locally high in the area between M'diq and Al Hoceima Bay (Fig. 4C), where the Western Alboran Gyre is permanently present. According to the scores of the first and second principal components, which show patterns similar to those of the biomass of dinoflagellates and diatoms, respectively, we may infer that the gyre enhances the development of dinoflagellates while the upwelling originating from the northern Alboran Sea enhances the development of diatoms. We also notice from the PCA that diatoms and dinoflagellates are well separated, likely because of their different growth preferences. Heterotrophic dinoflagellates such as *Protoperidinium* spp., *Gyro-*

dinium spirale and *Noctulica scintillans* are associated with the second component and diatoms such as *Nitzschia* spp. are associated with the first component. The coherent geographical distribution of the scores indicates that other parameters may have influenced the variability of microphytoplankton species.

We observed the highest biomass in the stretch between Cape Three Forks and Al Hoceima Bay. This area is highly influenced by upwelled water originating in the northern Alboran Sea that follow the Atlantic meandering jet and branches of the Western Alboran Gyre, enhancing the phytoplankton biomass. This is also an area of high species richness contributing to the general trend of increasing phytoplankton biodiversity with increasing production while lower species richness induced lower production. This means that biomass is related strongly to species richness and somewhat more weakly to ecological diversity. Agawin *et al.*, 2000 suggested that high biodiversity is typical in the Mediterranean Sea because of the wide range of climatic and hydrological conditions, which provide suitable conditions for temperate or subtropical organisms originating from the Atlantic Ocean. With its highly dynamic conditions, the Alboran Sea is thus an area where biodiversity is high.

The other parameters associated with diversity are mixed-layer depth and longitude (Supplementary Table S5). Larger mixed-layer depths ensure higher concentrations of nutrients from deeper water masses to fuel phytoplankton growth, which could trigger a phytoplankton succession characterized by lower diversity (Margalef, 1958; Agawin *et al.*, 2000). The longitudinal trend is related to decreasingly stable water mass conditions westward, favouring higher diversity.

Massive blooms (by Irigoien *et al.*, 2004) of a single or a few phytoplankton species decrease ecological diversity. Because of the relatively oligotrophic conditions of the Mediterranean, these conditions are rarely met except in strict littoral waters. Our data showed that this exception occurs near the Mar Chica lagoon, east of Cape Three Forks, where large blooms of the diatoms *Chaetoceros*, *Pseudo-nitzschia* and *Nitzschia longissima* were observed, with consequent decreases in ecological diversity. The Alboran Sea is the most productive open ocean waters of the oligotrophic Mediterranean where diversity is maximized.

Here we show that coastal waters of the southwestern Mediterranean tend to have a relatively homogeneous chlorophyll distribution between surface and depth layers, while open waters show clearly larger chlorophyll values at the surface than in deeper waters, due to a pronounced stratification. This trend is the opposite for microphytoplankton, whose biomass is higher in coastal areas near the surface than at depth, while in open waters no statistically significant difference is found between surface and deep waters. Species richness and Shannon diversity are always higher in surface waters (Table 1). Our results are in accordance with our first hypothesis that increasing hydrodynamics in the open ocean tends to increase diversity and microphytoplankton biomass. In line with our second hypothesis, coastal areas with

large terrestrial nutrient loads enhance large biomass in specific areas and favour the growth of certain taxa, reducing ecological diversity but not the species richness. In this case, it seems that biomass is strongly associated with species richness, while ecological diversity changes with cross-shore and longitudinal gradients. These findings emphasize that both diversity and dominance effects are important determinants in ecosystem processes, along with biomass production.

Conclusion

In conclusion, we have shown that the trends between phytoplankton diversity and biomass found in Irigoien *et al.*, 2004 are also valid for the southern Alboran Sea. These authors showed an increase in diversity (clearly reflected by species richness) with microphytoplankton biomass, as expected in oligotrophic waters. Only a few eutrophicated locations with high chlorophyll concentrations depart from this rule. The southern Alboran Sea is a very dynamic region of the Mediterranean that is strongly influenced by Atlantic waters and with diverse hydrodynamic conditions that make it a highly interesting area to study microphytoplankton composition and dynamics, especially in relation to climate and water mass trends. Though data on these topics are crucial for the understanding of the southwestern Mediterranean fisheries and their future trends, very little information is available. This study contributes to the incipient research on microphytoplankton in the region. We show that Cape Three Forks can be considered a longitudinal transition between a western area that is more influenced by Atlantic waters and an eastern area that has a greater Mediterranean influence.

Acknowledgements

This study was carried out in the context of the Pelagic Ecosystem Monitoring Programme and was supported by the National Institute of Fisheries Research (INRH) of Morocco. We would like to thank the programme coordinators and the entire team that participated in the survey aboard the Moroccan research vessel *Al Amir Moulay Abdellah*. Part of the manuscript was written during a placement funded by the Partnership for Observation of the Global Ocean and the Scientific Committee on Oceanic Research (POGO-SCOR) fellowship programme. We also thank Dr Elisa Berdalet for a critical review of the manuscript.

References

- Agawin, N.S.R., Duarte, C.M., Agustí, S., 2000. Nutrient and temperature control of the contribution of picoplankton to phytoplankton biomass and production. *Limnology and Oceanography*, 45 (3), 591-600.
- Arndt, E., Schembri, P., 2015. Common traits associated with

- establishment and spread of Lessepsian fishes in the Mediterranean Sea. *Marine Biology*, 162 (10), 2141-2153.
- Alcaraz, M., Calbet, A., Isari, S., Irigoien, X., Trepát, I. *et al.*, 2016. Variability of mesozooplankton biomass and individual size in a coast-offshore transect in the Catalan Sea: relationships with chlorophyll a and hydrographic features. *Scientia Marina*, 80 (S1), 79-87.
- Aleem, A.A., 1972. Effect of river outflow management on marine life. *Marine Biology*, 15, 200-208.
- Arin, L., Anxelu, X., Morán, G., Estrada, M., 2002. Phytoplankton size distribution and growth rates in the Alboran Sea (SW Mediterranean): short-term variability related to mesoscale hydrodynamics. *Journal of Plankton Research*, 24 (10), 1019-1033.
- Coll, M., Piroddi, C., Steenbeek, J., Kaschner, K., Lasram F.B.R. *et al.*, 2010. The Biodiversity of the Mediterranean Sea: Estimates, patterns, and threats. *PLoS ONE*, 5 (8), e11842.
- Dajoz, R. (Ed.), 2000. *Précis d'écologie*. Edition Dunod. Paris, 640 pp.
- Daoudi, M., Serve, L., Rharbi, N., El Madani, F., Florence, V., 2012. Phytoplankton distribution in the Nador lagoon (Morocco) and possible risks for harmful algal blooms. *Transitional Waters Bulletin*, 6 (1), 4-19.
- Demarcq, H., Somoue, L., 2015. Phytoplankton and primary productivity off Northwest Africa. In: *Oceanographic and biological features in the Canary Current Large Marine Ecosystem*. Valdés, L., Déniz-González, I. (Eds). IOC-UNESCO, IOC Technical Series, Paris.
- Duarte, P., Macedo, M. F., Cancela da Fonseca, L., 2006. The relationship between phytoplankton diversity and community Function in a coastal Lagoon. In: *Marine Biodiversity: Patterns and Processes, Assessment, Threats, Management and Conservation*. Martens, K., Queiroga, H., Cunha, M. R., Cunha, A., Moreira, M. H. *et al.*, (Eds). Developments in Hydrobiology, Netherlands.
- Elghrib, H., Somoue, L., Elkhiahi, N., Berraho, A., Makaoui, A. *et al.*, 2012. Phytoplankton distribution in the upwelling areas of the Moroccan Atlantic coast localized between 32°30'N and 24°N. *Comptes Rendus Biologies*, 335 (8), 541-554.
- Escudier, R., Clementi, E., Omar, M., Cipollone, A., Pistoia, J. *et al.*, 2020. Mediterranean Sea physics reanalysis (CMEMS MED-Currents) (Version 1) [Data set]. *Copernicus Monitoring Environment Marine Service (CMEMS)*.
- Estrada, M., Dolors, B., 1979. Two phases of the phytoplankton community in the Baja California Upwelling. *Limnology and Oceanography*, 24 (6), 1065-1080.
- Estrada, M., 1982. Ciclo anual del fitoplancton en la zona costera frente a Punta Endata (Golfo de Vizcaya). *Investigación Pesquera*, 46 (3), 469-491.
- Estrada, M., 1996. Primary production in the northwestern Mediterranean. *Scientia Marina*, 60 (Supl. 2), 55-64.
- Falkowski, P.G., Oliver, M.J., 2007. Mix and match: how climate selects phytoplankton. *Nature Reviews Microbiology*, 5, 813-819.
- Gómez-Jakobsen, F.J., Mercado, J.M., Cortés, D., Yebra, L., Salles, S., 2019. A first description of the summer upwelling off the Bay of Algeciras and its role in the northwestern Alboran Sea. *Estuarine, Coastal Shelf Science*, 225, 106230.
- Hulbert, E.M., 1963. The diversity of phytoplanktonic populations in oceanic, coastal and estuarine regions. *Journal of Marine Research*, 21, 81-93.
- IPBES, 2019. *Summary for policymakers of the global assessment report on biodiversity and ecosystem services of the Intergovernmental Science-Policy Platform on Biodiversity and Ecosystem Services*. Díaz S, Settele J, Brondizio ES, Ngo HT, Guèze M, *et al.*, (Ed.), IPBES secretariat, Bonn, Germany, 56 pp.
- Irigoien, X., Huisman, J., Harris, R.P., 2004. Global biodiversity patterns of marine phytoplankton and zooplankton. *Nature*, 429, 863-867.
- Iversen, K.R., Primicerio, R., Larsen, A., Egge, J.K., Peters, F. *et al.*, 2010. Effects of small-scale turbulence on lower trophic levels under different nutrient conditions. *Journal of Plankton Research*, 32, 197-208.
- Linder, S., 1974. A proposal for the use of standardized methods for, chlorophyll determinations in ecological and eco-physiological investigations. *Physiologia Plantarum*, 32 (2), 154-156.
- Margalef, R., 1958. *Temporal Succession and Spatial Heterogeneity in Natural Phytoplankton*. Perspectives in Marine Biology. University of California Press, USA, 323-350 pp. <https://digital.csic.es/handle/10261/165671>
- Margalef, R., 1999. The play of diversity/biodiversity in the construction of the biosphere, as exemplified in the Mediterranean phytoplankton and as expression of the operation of very general principles. *Journal of Mediterranean Ecology*, 1, 3-10.
- Menden-Deuer, S., Lessard, E. J., 2000. Carbon to volume relationships for dinoflagellates, diatoms, and other protist plankton. *Limnology and Oceanography*, 45, 569-579.
- Mercado, J.M., Ramírez, T., Cortés, D., Sebastián, M., Vargas-Yáñez, M., 2005. Seasonal and inter-annual variability of the phytoplankton communities in an upwelling area of the Alborán Sea (SW Mediterranean Sea). *Scientia Marina*, 69, 451-465.
- Pavaux, A., Berdalet, E., Lemée, R., 2020. Chemical ecology of the benthic dinoflagellate genus *Ostreopsis*: Review of Progress and Future Directions. *Frontiers in Marine Science*, 7, 498.
- Pavlovskaya, T.V., Kondratyeva, T.M., 1981. Carbon content dependence on the cells' volume of the mass phytoplankton species from the Black Sea (in Russian). *Okeanologia*, 21, 523-528.
- Rijal Leblad, B., Lundholm, N., Goux, D., Veron, B., Sagou, R. *et al.*, 2013. Pseudo-Nitzschia Peragallo (Bacillariophyceae) diversity and Domoic Acid accumulation in Tuberculate Cockles and Sweet Clams in M'diq Bay, Morocco. *Acta Botanica Croatica*, 72 (1), 35-47.
- Rijal Leblad, B., Amnhir, R., Requia, S., Sitel, F., Daoudi, M. *et al.*, 2020. Seasonal variations of phytoplankton assemblages in relation to environmental factors in Mediterranean coastal Waters of Morocco, a focus on HABs species. *Harmful Algae*, 96, 101819.
- Sathyendranath, S., Stuart, V., Nair, A., Oka, K., Nakane, T. *et al.*, 2009. Carbon-to-chlorophyll ratio and growth rate of phytoplankton in the sea. *Marine Ecology Progress Series*, 383, 73-84.
- Scales, K.L., Miller, P.I., Hawkes, L.A., Ingram, S.N., Sims,

- D.W. *et al.*, 2014. On the Front Line: frontal zones as priority at-sea conservation areas for mobile marine vertebrates. *Journal of Applied Ecology*, 51 (6), 1575-1583.
- Schneider, C.A., Rasband, W. S., Eliceiri, K. W., 2012. NIH Image to ImageJ: 25 years of image analysis. *Nature Methods*, 9, 671-675.
- Shannon, C., Wiener, E. (Ed.), 1949. *The Mathematical Theory of Communications*. Illinois Press, Urbana, 379-423 pp.
- Tester, P.A., Litaker, R.W., Berdalet, E., 2020. Climate change and harmful benthic microalgae. *Harmful Algae*, 91, 101655.
- Üthermühl, H., 1958. Zur Vervollkommnung der quantitativen Phytoplankton Methodik. *Mitteilungen Internationale Vereinigung für theoretische und angewandte Limnologie*, 91-38.
- Vadrucci, M.R., Cabrini, M., Basset, A., 2007. Biovolume determination of phytoplankton guilds in transitional water ecosystems of Mediterranean Ecoregion. *Transitional Waters Bulletin*, 2, 83-102.
- Vargas-Yáñez, M., Plaza, F., Garcia-Lafuente, J., Sarhan, T., Vargas, J.M. *et al.*, 2002. About the seasonal variability of the Alboran Sea circulation. *Journal of Marine Systems*, 35, 229-248.

Supplementary Data

The following supplementary information is available online for the article:

Fig. S1: Chlorophyll a concentration (logarithmic scale) from the MODIS sensor on 17 April 2018. The 200 m isobath is superimposed.

Table S1. Information on sampling stations during the cruise. Chlorophyll and phytoplankton data were collected and analysed at all stations.

Table S2. Occurrence of the 106 taxa along the Moroccan Mediterranean Coast.

Table S3. Relative abundances of the 17 highly abundant taxa of microphytoplankton in surface and deep layers along the Mediterranean coast of Morocco in April 2018

Table S4. Longitudinal comparison of the relative abundances of the main dominant taxa. Taxa were selected on the basis of relative abundances that were higher than 4 % and occurred simultaneously in both regions separated by Cape Three Forks and in both depth layer.

Table S5. Statistical summary of stepwise multiple regression analyses for diversity variables.